Structural Characteristics of Homogeneous Hydrophobic Ionic Liquid–HNO_3–H_2O Ternary System: Experimental Studies and Molecular Dynamics Simulations

Jing Fu,[†] Y. Isaac Yang,[‡] Jun Zhang,[‡] Qingde Chen,[†] Xinghai Shen,*[,†] and Yi Qin Gao*[,‡]

[†]Beijing National Laboratory for Molecular Sciences (BNLMS), Fundamental Science on Radiochemistry and Radiation Chemistry Laboratory, College of Chemistry and Molecular Engineering, Peking University, Beijing 100871, PR China

[‡]Beijing National Laboratory for Molecular Sciences (BNLMS), Institute of Theoretical and Computational Chemistry, College of Chemistry and Molecular Engineering, Peking University, Beijing 100871, PR China

ABSTRACT: The solubility of water in the hydrophobic ionic liquid 1-ethyl-3-methylimidazolium bis-(trifluoromethylsulfonyl)imide ($[C_2mim][NTf_2]$) increases significantly in the presence of HNO_3. $[C_2mim][NTf_2]$ is completely miscible with HNO_3 but immiscible with water. The triangular phase diagram of the ternary system $[C_2mim][NTf_2]$–HNO_3–H_2O was determined at 300.1 K. The homogeneous $[C_2mim][NTf_2]$–HNO_3–H_2O phase is thermodynamically stable, while it can be separated into two phases with an increase of water content. Experiments (electrospray ionization mass spectrometry, Fourier transform infrared spectrometry, and ^{1}H-nuclear magnetic resonance spectrometry) and molecular dynamics simulations were carried out to investigate the interaction between $[C_2mim][NTf_2]$, HNO_3, and water in the homogeneous phase. It was found that NO_3^- ions interact with both C_2mim^+ and water via H-bonding and act as a "bridge" to induce a large amount of water to be dissolved in the hydrophobic IL phase. This confirms that the complexes $[C_2mim–NTf_2–C_2mim]^+$ and $[NTf_2–C_2mim–NTf_2]^-$ exist in the homogeneous $[C_2mim][NTf_2]$–HNO_3–H_2O system at the concentration of HNO_3 up to 27.01 wt % and of water as high as 20.74 wt %.

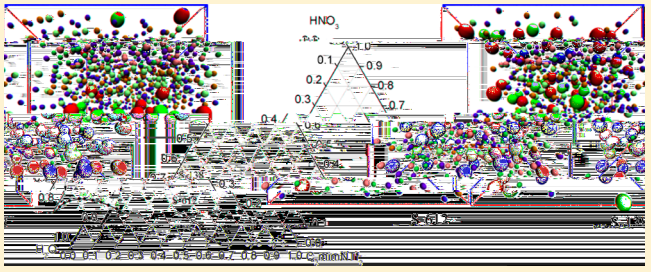

1. INTRODUCTION

Ionic liquids (ILs) are regarded as excellent solvents in various chemical reactions and separation processes for their specific properties (such as general nonflammability, high thermal stability, wide liquid range, and negligible vapor pressure).[1−3] The physicochemical properties such as viscosity, electrical conductivity, solvating ability, and the microstructures of ILs are affected significantly by impurities, and water as the most common impurity in both hydrophilic and hydrophobic ILs has attracted much attention.[4−8]

Hydrophilic ILs can be easily dissolved in water. The molecular state of water in a hydrophilic IL varies with the increase of water content and the microstructure of an IL is also changed by the addition of water. For instance, 1-dodecyl-3-methylimidazolium bromide ($[C_{12}mim]Br$) and 1-decyl-3-methylimidazolium bromide ($[C_{10}mim]Br$) form lyotropic liquid-crystalline phases in the presence of water and exhibit different phase behaviors as the water content increases.[9,10]

Hydrophobic ILs are immiscible with water. One of the most common uses of hydrophobic ILs is in liquid−liquid extraction,[11,12] where ILs are usually considered as next generation diluents in replacement of volatile organic solvents (VOCs), especially in the reprocessing of spent nuclear fuel.[13,14] However, because some phase equilibria exist between the aqueous phase and the IL phase, the composition of the aqueous phase could affect the IL phase directly. Some extraction studies revealed that HNO_3 in the aqueous phase is partly transferred to the $[C_4mim][NTf_2]$ phase during the extraction.[11,15,16] The water solubility in $[C_4mim][NTf_2]$ can increase to ca. 32000 ppm (about 2.5 mol L^{-1}) in the presence of HNO_3 at 7.5 mol L^{-1}.[17] Gaillard et al.[18] investigated the extraction of HNO_3, $HReO_4$, $HClO_4$, and HCl to the $[C_4mim][NTf_2]$ phase over a wide range of acid concentrations in the aqueous phase and examined the effect of tributylphosphate (TBP) as co-solvent. In the biphasic system, they found that TBP has great influence on the water−IL miscibility. TBP can promote the transfer of C_4mim^+ ions to the aqueous phase as the acid concentration increases, which indicates that the IL phase extracts a certain amount of water and acid from the aqueous phase.

mutual miscibility of water and $[C_4mim][NTf_2]$, causing either salting-in or salting-out effects.[20]

However, the investigation of the effect of water on the structures of hydrophobic ILs has so far been mainly focused on the usage of a small amount of water. As is known, an IL containing the anion bis(trifluoromethylsulfonyl)imide (NTf_2^-) is usually hydrophobic. The saturated water content of $[C_2mim][NTf_2]$ is lower than 2 wt % in equilibrium with air or aqueous phase at room temperature.[6] The molecular state of water exists as symmetric 1:2 H-bonded complexes with NTf_2^- based IL, i.e., anion···HOH···anion at the water content below saturation, while the interaction of water with the IL cation plays a minor role.[21,22] Koddermann et al. utilized FTIR spectroscopy and density functional calculations (DFT) to show that water molecules are mainly H-bonded to the anions of $[C_2mim][NTf_2]$ in two configurations. One type of water molecules forms two H-bonds to two anions, and the other forms a strong single H-bond to an anion at the water content below 1 wt %.[6]

HNO_3 as a specific chemical compound can adjust the hydrophobicity of the imidazolium family ionic liquids. The structure of a hydrophobic IL should be influenced by the presence of HNO_3 and water. However, there is no direct study about the monophase behavior among HNO_3, water, and the IL. The state of water and HNO_3 in the IL phase is not yet to be understood at the molecular level. Therefore, in this article, we aim to examine the interaction of HNO_3, water, and hydrophobic IL as well as the structural characteristics in the homogeneous ternary systems based on experimental methods and molecular dynamics simulations.

2. EXPERIMENTAL SECTION

2.1. Materials. We found that the solubility of water in $[C_nmim][NTf_2]$ (n = 2, 4, 6, 8, 10, 12) increases significantly when HNO_3 exists, and all molecules can form the homogeneous systems of IL−HNO_3−H_2O. Because of relatively low viscosity, $[C_2mim][NTf_2]$, as shown in Scheme 1, is one of the preferred ionic liquids used in the extraction system. Therefore, $[C_2mim][NTf_2]$ is selected as the representative to investigate the structural characteristics of hydrophobic IL−HNO_3−H_2O systems.

Scheme 1. Structure of $[C_2mim][NTf_2]$

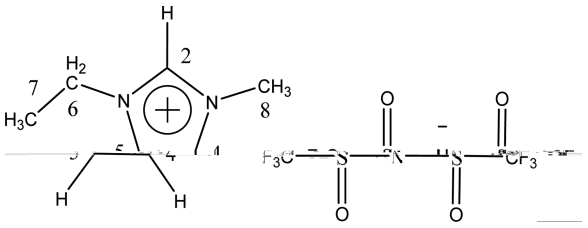

$[C_2mim][NTf_2]$ (>99%) was prepared according to ref 23 and was identified by ^1H nuclear magnetic resonance (^1H NMR) and electrospray ionization mass spectrometry (ESI/MS). The IL was dried in vacuum (about 1 Pa) at 343 K for over 48 h. Water content in $[C_2mim][NTf_2]$ was less than 300 ppm, as determined by Karl Fischer titration (Mettler Toledo, Switzerland). Nitric acid of analytical grade was purchased from Beijing Chemical Plant and was used without further treatment. Water content in HNO_3 was determined by Karl Fischer titration. Tridistilled water was used in this study.

2.2. Apparatus. The water contents of the monophasic mixtures were determined by Karl Fischer titration. The compositions of samples are listed in Table 1 and shown in Figure 1, which were calculated by weight. The mass spectra of the $[C_2mim][NTf_2]$−HNO_3−H_2O monophasic mixtures were measured by ESI/MS on a Fourier transform ion cyclotron resonance mass spectrometer, APEX IV (Bruker, USA). Fourier

Table 1. Compositions of Monophasic Samples (Mole Fraction)

	$[C_2mim][NTf_2]$	HNO_3	H_2O
Series I $[C_2mim][NTf_2]$−HNO_3−H_2O			
1	0.90	0.03	0.07
2	0.82	0.06	0.12
3	0.75	0.08	0.17
4(S-612)	0.69	0.10	0.21
Series I′ $[C_2mim][NTf_2]$−H_2O			
1′	0.93	0	0.07
2′	0.88	0	0.12
3′	0.83	0	0.17
4′	0.77	0	0.23
Series II $[C_2mim][NTf_2]$−HNO_3−H_2O			
1	0.42	0.16	0.42
2	0.26	0.20	0.54
3	0.19	0.22	0.59
4	0.12	0.24	0.64
5	0.09	0.25	0.66
6(S-138)	0.08	0.25	0.67

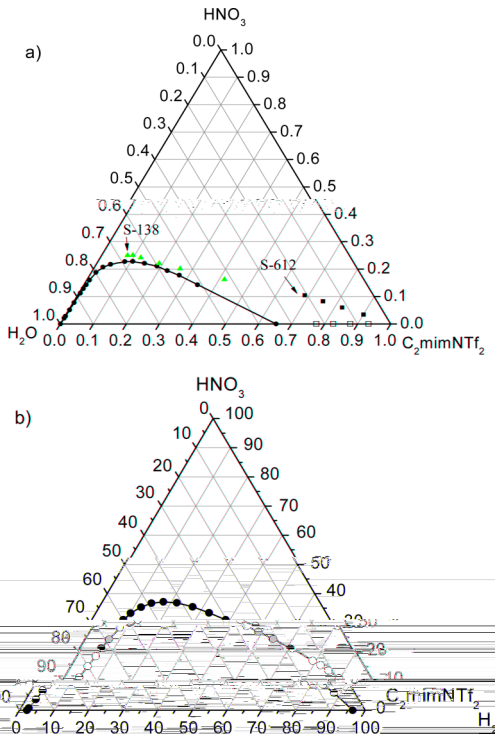

Figure 1. Triangular phase diagrams for ternary compositions of $[C_2mim][NTf_2]$ with HNO_3 and H_2O plotted as mole fraction (a) and as initial wt % (b), respectively, determined at 300.1 ± 0.1 K. The region extending from IL−HNO to H_2O apex is a monophase containing all three components. The compositions of series I (■), series I′ (□), and series II (▲) are shown in (a) and listed in Table 1.

DOI: 10.1021/acs.jpcb.6b01214
J. Phys. Chem. B 2016, 120, 5194−5202

transform infrared spectroscopy (FTIR) spectra of the monophasic mixtures were obtained by a Bruker Vector 22 spectrometer at a frequency ranging from 400 to 4000 cm^{-1} with a resolution of 1 cm^{-1}. To prevent the volatilization of water during the measurement, the KBr liquid bath was used in all measurements. ^1H NMR spectra of the monophasic mixtures were recorded on a Bruker AV400 MHz NMR spectrometer with chloroform-d (>99.8% D atom, Innochem) as the external standard.

2.3. Methods. *2.3.1. Ternary Phase Diagrams.* The ternary phase diagram of $[C_2mim][NTf_2]$−HNO_3−H_2O was determined by visual detection at 300.1 ± 0.1 K. The sample in glass cell was immersed in a thermostatic bath at 300.1 ± 0.1 K and was continuously stirred to sufficiently reach equilibrium. Boundary points were obtained by cloud-point titration of samples containing known water−IL weight compositions with accurately measured nitric acid content and known HNO_3−IL weight compositions with water. The measurement results were reproducible within an error of ±0.1%.

2.3.2. Simulations. All simulations were performed using AMBER 9 software package[24] with NPT ensemble at 300 K and 1 atm. The force field parameters of C_2mim^+ were taken from Andrade et al.,[25] while those of NTf_2^- were from Lopes and Pádua.[26] In our simulations, the hypothetical models of HNO_3 fully dissociated to H_3O^+ and NO_3^- ions, with the force field parameters developed by Baaden et al. being used.[27] To be consistent with the force field parameters of HNO_3, we used the TIP3P model (model F[25]) to represent the water molecules. The SHAKE[28] algorithm was employed to constrain all bonds including hydrogen, while all simulations utilized a 2 fs time step. A cutoff of 10 Å was used for the short-range forces.

We chose two monophasic systems to perform the simulations. One system has a molar ratio of IL:HNO_3:water = 0.08:0.25:0.67 (hereinafter called S-138), which is close to the coexistence line on the ternary phase diagram (Figure 1a). There are 64 pairs of IL molecules, 192 pairs of H_3O^+ and NO_3^- ions, and 352 water molecules in this system. The other system has a molar ratio of IL:HNO_3:water = 0.69:0.10:0.21 (hereinafter called S-612), lying in the monophasic zone of the ternary phase diagram (Figure 1a). There are 125 pairs of IL molecules, 20 pairs of H_3O^+ and NO_3^- ions, and 20 water molecules.

We calculated λ following the definition by Wipff et al.:[29] the whole periodic box was split into 64 boxes of equal sizes, and in each box i we calculated $d_{j,i}$, the density of species j in box i, and $1/d_i = \sum 1/d_{j,i}$. Then the demixing index λ was obtained by normalizing the average value of all d_i: $\lambda = 1/N\langle d_i\rangle$, where the normalization factor N was calculated by the density of species j in the whole system (D_j): $1/N = \sum 1/D_j$. We used the VMD[30] software package for the visualization of molecular structures.

3. RESULTS AND DISCUSSION

3.1. Triangular Phase Diagram. Ternary mixtures of HNO_3 and water with $[C_2mim][NTf_2]$ were studied to determine the range of miscibility of the phases. The $[C_2mim][NTf_2]$−HNO_3−H_2O triangular phase diagrams at 300.1 ± 0.1 K are shown in mole ratios (Figure 1a) and initial weight ratios (Figure 1b). The triangular phase diagrams display the characteristics of a typical three-component system containing two miscible component pairs ($[C_2mim][NTf_2]$ and HNO_3, HNO_3 and water) and one immiscible component pair ($[C_2mim][NTf_2]$ and water). The miscibility of water in the IL increased with an increase in the concentration of HNO_3 so that a monophasic system containing large water content was obtained.

On the addition of water, the monophasic system gradually became a biphasic system containing the IL-rich phase and the aqueous-rich phase. Comparing the IL-rich phase with $[C_2mim][NTf_2]$ saturated only with water, we found that water contents were both 2.1 wt % at 292.5 K using Karl Fischer titration. The element analyses showed that the compositions of the IL-rich phase and the $[C_2mim][NTf_2]$ only saturated with water were almost identical. In the IL-rich phase, there were 10.56 wt % of N, 24.13 wt % of C, and 2.89 wt % of H. In $[C_2mim][NTf_2]$ only saturated with water, there were 10.51 wt % of N, 24.13 wt % of C, and 2.91 wt % of H. The observed signals of the IL-rich phase and the $[C_2mim]$-$[NTf_2]$ only saturated with water were almost the same based on ESI/MS spectrum and ^1H NMR (figures not shown). These results indicate that the composition of the IL-rich phase separated from the $[C_2mim][NTf_2]$−HNO_3−H_2O system is the same as that of $[C_2mim][NTf_2]$ only saturated with water. Such an observation shows that the interaction between HNO_3 and IL is very weak and the miscible process is reversible.

3.2. Experimental Measurements. *3.2.1. ESI/MS.* As an effective method for studying the composition of noncovalent complexes, ESI/MS was applied to determine the complex composition in this work. We chose two homogeneous mixture samples S-138 and S-612, which are listed in Table 1 and shown in the triangular phase diagram (Figure 1a), to investigate the microstructure of the $[C_2mim][NTf_2]$−HNO_3−H_2O monophasic system. The ESI/MS results of S-138 are shown in Figure 2a,b. The positive signal at 502.1 and the negative signal at 670.9 can be observed, which correspond to the cationic complex $[C_2mim{-}NTf_2{-}C_2mim]^+$ and the anionic complex $[NTf_2{-}C_2mim{-}NTf_2]^-$, respectively. These signals exist in the ESI/MS spectrum of pure $[C_2mim][NTf_2]$ as well (Figure not shown). It is worth noting that the positive signal of 284.2 corresponds to the cationic complex $[C_2mim{-}NO_3{-}C_2mim]^+$. Despite the weak relative intensity, the signal at 284.2 proves that in the three-component homogeneous system, NO_3^- can interact directly with C_2mim^+. However, in the negative ion mass spectra, the signals representing the complexes $[NO_3{-}C_2mim{-}NO_3]^-$ or $[NO_3{-}C_2mim{-}NTf_2]^-$ do not appear. This result shows that although the concentration of HNO_3 is up to 27.01 wt % and the water content is as high as 20.74 wt % in the system, the major complexes are still $[C_2mim{-}NTf_2{-}C_2mim]^+$ and $[NTf_2{-}C_2mim{-}NTf_2]^-$, and a few NO_3^- ions substitute the position of NTf_2^- ions. The above results indicate that the main interaction is between C_2mim^+ and NTf_2^- in the $[C_2mim]$-$[NTf_2]$−HNO_3−H_2O homogeneous mixture. HNO_3 and water only slightly perturbs the major complexes between C_2mim^+ and NTf_2^-.

The ESI/MS results of S-612 are shown in Figure 2c,d. The positions of signals are almost the same as those for S-138. The intensity of the signal at 284.2 is not much different from that of S-138. Meanwhile, the intensity of the signal at 670.9 for S-612, which corresponds to the anionic complex $[NTf_2{-}C_2mim{-}NTf_2]^-$, is weakened remarkably as compared with that of S-138. Such a finding implies that the interaction between NTf_2^- and C_2mim^+ becomes weaker, which indicates that the strength of the interaction among NO_3^-, C_2mim^+, and NTf_2^- depends on the composition of the system. In addition, these observations show that $[C_2mim][NTf_2]$ has good

DOI: 10.1021/acs.jpcb.6b01214
J. Phys. Chem. B 2016, 120, 5194−5202

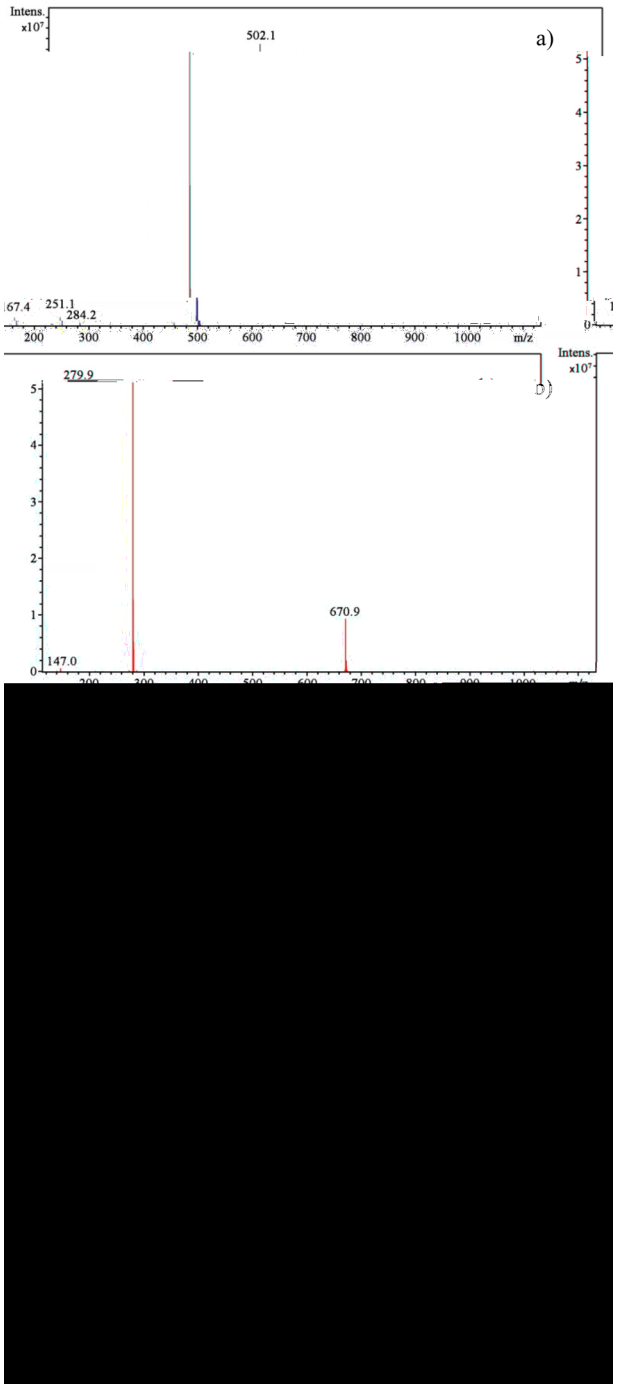

Figure 2. ESI spectra of monophasic $[C_2mim][NTf_2]$–HNO_3–H_2O mixtures. (a) Positive and (b) negative ESI spectra of S-138, (c) positive and (d) negative ESI spectra of S-612.

resistance to oxidation, which is of importance for the IL based extraction phase to extract metal ions from an aqueous phase with high acidity.

3.2.2. FTIR. The effect of HNO_3 on the existing state of water in $[C_2mim][NTf_2]$ was investigated by FTIR, and the results are given in Figure 3. We compared $[C_2mim][NTf_2]$–HNO_3–H_2O (series I) with $[C_2mim][NTf_2]$–H_2O (series I′) monophasic mixtures. Compositions of these two systems containing the same water content are listed in Table 1 and shown in Figure 1a. Figure 3a shows the vibrational bands of –OH in $[C_2mim][NTf_2]$–HNO_3–H_2O (series I) with $[C_2mim][NTf_2]$–H_2O (series I′) monophasic mixtures. In $[C_2mim][NTf_2]$–H_2O systems, two vibrational peaks are clearly observed at ca. 3560 and 3640 cm^{-1} (series I′, dash line), respectively. They can be assigned to symmetric (ν_s) and antisymmetric (ν_{as}) stretching peaks of isolated water.[6] It has been reported in the literature that when the water content is less than the saturation limit in $[C_2mim][NTf_2]$, the state of water can be assigned as isolated water molecules interacting via H-bonding with NTf_2^-.[22,31] However, in $[C_2mim][NTf_2]$–HNO_3–H_2O systems (Figure 3a, series I, solid line), the vibrational bands of –OH red-shift remarkably and broaden as well. The peaks of ν_s(–OH) and ν_{as}(–OH) can still be distinguished into two bands at ca. 3556 and 3625 cm^{-1}, respectively. This phenomenon indicates that water in homogeneous $[C_2mim][NTf_2]$–HNO_3–H_2O systems can be still regarded as isolated water. Moreover, it is worth noting that as the concentration of HNO_3 increases, the intensity of the peak of ν_s(–OH) becomes higher than that of ν_{as}(–OH) in $[C_2mim][NTf_2]$–HNO_3–H_2O systems, and the two peaks have a tendency to form a broaden peak and shift to a lower wavenumber. In the literature, it was suggested that water molecule interacts with anion via hydrogen bond in C_nmim^+ based IL, while the interaction of water with the IL cation plays a minor role.[6,21,22,32] The result of ESI/MS analysis indicates that a few NO_3^- ions substitute the position of NTf_2^- ions. Therefore, we can infer that water prefers to interact with NO_3^- via hydrogen bond in the $[C_2mim][NTf_2]$–HNO_3–H_2O system, which may make the intensity of the peak of ν_s(–OH) higher than that of ν_{as}(–OH).

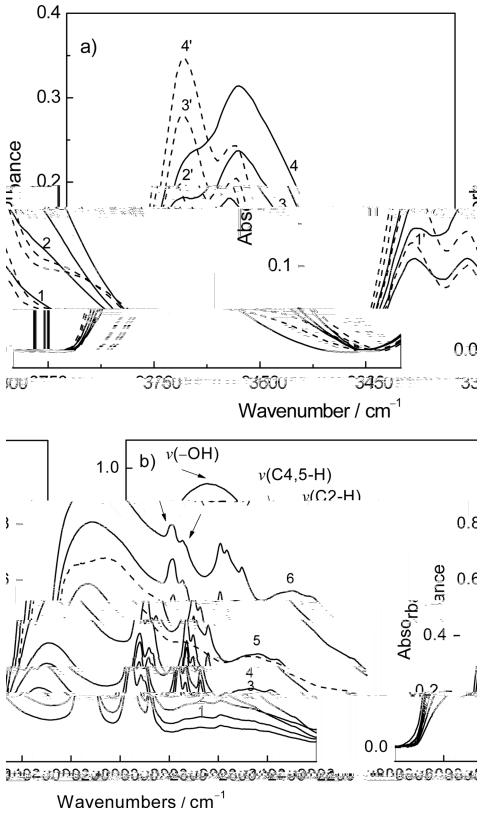

Figure 3. IR spectra of (a) $[C_2mim][NTf_2]$–HNO_3–H_2O samples (series I, solid line) and $[C_2mim][NTf_2]$–H_2O samples (series I′, dash line), and (b) $[C_2mim][NTf_2]$–HNO_3–H_2O samples (series II) and 68 wt % HNO_3 (dash line).

DOI: 10.1021/acs.jpcb.6b01214
J. Phys. Chem. B 2016, 120, 5194–5202

In Figure 3b, one can find that as the water content is higher than 2 wt % in the $[C_2mim][NTf_2]$–HNO_3–H_2O systems (series II), the absorption bands of –OH become broaden and move to the lower wavenumber. Figure 3b shows that the vibrational bands of –OH at ca. 3538 cm^{-1} move to ca. 3465 cm^{-1}, close to that of 68 wt % HNO_3 at ca. 3430 cm^{-1}, with an increase of water and HNO_3 contents in the $[C_2mim][NTf_2]$–HNO_3–H_2O systems. These spectral features mean that when the water content increases, the isolated water gradually turns into the bulk water. Moreover, the vibrational bands at ca. 3158 cm^{-1} and ca. 3121 cm^{-1} are attributed to C4–H, C5–H, and C2–H stretching vibrations on the imidazolium ring.[31] As the concentration of HNO_3 and water increase, one can observe a blue-shift of C4–H and C5–H from 3158 to 3166 cm^{-1}, while C2–H vibration only shifts from 3121 to 3123 cm^{-1}, implying that the C4–H, C5–H, and C2–H can interact with NO_3^-. In the literature, it was suggested that the C2–H of C_2mim^+ interacts with anion via hydrogen bond and electrostatic interaction.[6,32] Noack et al.[31] found that the interaction between C4–H, C5–H, and anion became important when the C2 position was methylated. In the $[C_2mim][NTf_2]$–HNO_3–H_2O systems, the C2–H may only interact with one O atom of NO_3^-, while C4–H and C5–H with two O atoms of one NO_3^- simultaneously. This may be the reason that the force constant change of C4–H and C5–H is more serious than that of C2–H.

3.2.3. ^1H NMR. In $[C_2mim][NTf_2]$–HNO_3–H_2O monophasic systems, the state of C_2mim^+ can be further tested by ^1H NMR. Figure 4a shows that the chemical shifts of the protons of C_2mim^+ all move to downfield as the concentrations of water and HNO_3 increase in series II. In Figure 4a, we can find that the chemical shifts of C6–H, C7–H, and C8–H on the alkyl chain are increased to almost the same extent with increasing concentrations of HNO_3 and water. The chemical shifts of C2–H, C4–H, and C5–H on the imidazolium ring move to downfield as well, however, with obvious difference from those of the alkyl chain protons. Therefore, one can conclude that the chemical environment of protons on the imidazolium ring is different from that of the alkyl chain protons. Moreover, the increase of the chemical shift of C2–H is lower than those of C4–H and C5–H, similar to the blue-shift phenomenon of C–H stretching vibration of imidazolium ring in IR spectra. This may also be ascribed to the different interaction modes between NO_3^- and C(2, 4, 5)–Hs of imidazolium ring.

To evaluate the effect of HNO_3 on the C_2mim^+ and exclude the effect of water, we compared the chemical shift of protons of C_2mim^+ in series I with the corresponding ones in series I′. Figure 4b shows that the chemical shifts of individual hydrogen atoms in series I change very little as compared with that in series I′. As the concentration of HNO_3 increases, the chemical shifts of C6–H, C7–H, and C8–H on the alkyl chain are increased. However, the chemical shifts of C4–H and C5–H move to downfield slightly and that of C2–H even moves to high field mildly. In the pure $[C_2mim][NTf_2]$, the interaction between C_2mim^+ and NTf_2^- is dominated by H-bonding at the C2–H position on the imidazolium ring, besides the electrostatic attraction.[30] Therefore, the electron density of these three hydrogen atoms on the imidazolium ring is reduced by the existence of HNO_3 due to the strengthening of the hydrogen bonding. These results imply that in the $[C_2mim][NTf_2]$–HNO_3–H_2O monophasic systems, NO_3^- interacts mainly with the imidazolium ring by H-bonding at C2–H, C4–H, and C5–H.

3.3. Molecular Dynamics Simulations. To further investigate the effects of HNO_3 on increasing the miscibility of $[C_2mim][NTf_2]$ with water, all-atom molecular dynamics simulations were performed on the mixture of IL, HNO_3, and water at different concentrations. In our simulation, S-138 with saturated moisture evolves into two separated phases, and snapshots taken from the early and late stages of the simulation are shown in Figure 5. In the experiments, S-138 is a monophasic system, but its composition is close to the boundary line between the monophasic and the biphasic in the phase diagram (Figure 1a). The state of S-138 is sensitive to the change of the environment. Therefore, in the simulation, the gradual separation of the S-138 from monophase (Figure 5a) into a biphase (Figure 5b–d) can be expected. We then use the demixing index λ to monitor this process. The demixing index, which can range from one (fully mixed) to zero (completely separated), is a value used to characterize the mixability of several species. The system comprises of five molecular/ionic species: water, NO_3^- anions, H_3O^+ ions, NTf_2^- anions, and C_2mim^+ cations. To measure the mixability of different molecules and ions, we categorize the constituents in the following three different ways: (1) five subspecies, corresponding to all the fi

are the same) of the demixing process of the mixture of $[C_2mim][NTf_2]$ and water performed by Sieffert and Wipff.[33] Such a result is consistent with the effect of HNO_3 in promoting the association between IL and water molecules. After phase separation (Figure 5c,d), almost all the H_3O^+ and NO_3^- ions are located in the aqueous phase, indicating that the association of HNO_3 with water is preferred. Another phase is mainly composed of the IL and a few water molecules, and few H_3O^+ and NO_3^- ions appear in this phase. These results are consistent with the experimental observations, in which the monophasic system can separate into a biphasic one. In contrast, S-612 remains stable as a single phase in our simulation, and the change of demixing index of IL and non-IL molecules is negligible (Figure 6b). The increase of other two demixing indices at the first 100 ns simulation implies that

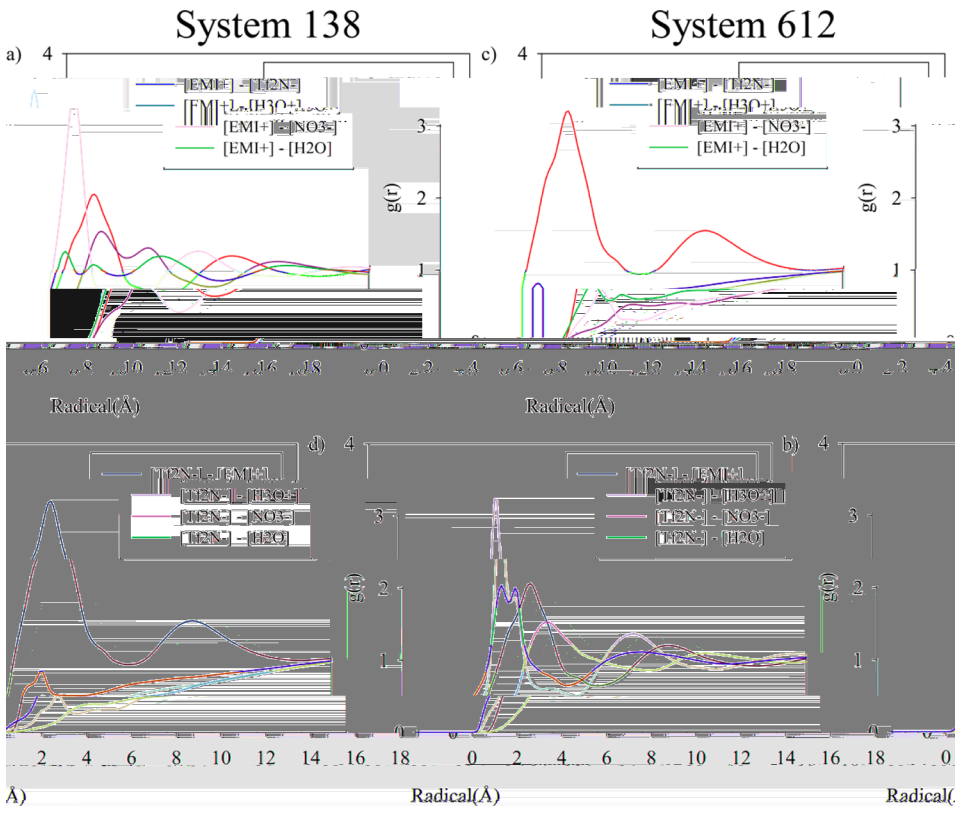

Figure 7. Radical distribution function (RDF) of different molecules around the IL ions in S-138 (a,b) and S-612 (c,d), respectively. When we calculated the RDFs, C_2mim^+ was represented by the mass center of the heavy atoms of imidazole ring, NTf_2^- as well as NO_3^- was represented by the nitrogen atom, and H_3O^+ as well as H_2O was represent by oxygen atom. The RDFs in S-138 are calculated from the MD trajectory after 200 ns (phase separation), and RDFs in S-612 are calculated from the MD trajectory after 100 ns.

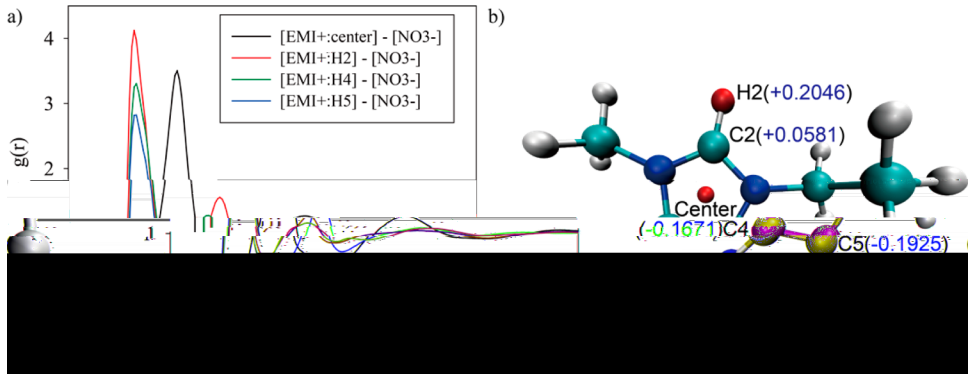

Figure 8. (a) Radical distribution functions (RDFs) of NO_3^- ions around the three different hydrogen atoms of C_2mim^+ in S-612. (b) The atom names and charges (the point charges used in force field) of C_2mim^+ used in the radical distribution function.

bridges them into close contact. Although the distributions of molecules around the NO_3^- ions are very different in the two systems (Figure 9a,b), the distributions of molecules around the NO_3^- ions are the same in the two systems: H_3O^+ > H_2O > C_2mim^+ > NTf_2^-. Moreover, as seen in Figure 9c,d, the two systems also share a same trend for the probabilities of finding a different particle in the vicinity of H_3O^+: H_2O/NO_3^- > NTf_2^- > C_2mim^+. This tendency indicates that both NO_3^- and H_3O^+ interact strongly with water molecules. As H_3O^+ and NO_3^- can easily mix into the IL through Coulombic interactions, NO_3^- allows the IL and water molecules to approach each other and increase their miscibility. On grounds of such inference, it is not surprising that the RDF peaks of water molecules around NO_3^- in the homogeneous S-612 are even higher than that in the phase-separated S-138. However, because the interaction between NO_3^- and water is much stronger than that between NO_3^- and IL, NO_3^- preferentially interacts with water molecules, especially when there are excess water molecules. When the percentage of water molecules reaches the miscibility limit, like in the case of S-138, a phase separation occurs (Figure 5). In this case, H_3O^+ or NO_3^- that can serve to associate water with the IL ions becomes insufficient and NO_3^- is largely buried in the bulk water.

According to the results of experiments and simulations, the $[C_2mim][NTf_2]$–HNO_3–H_2O monophasic systems show properties varying with the concentration of HNO_3 and water. When the molar ratio of water to HNO_3 is small, the IL and water are miscible. Under this condition, the interaction

DOI: 10.1021/acs.jpcb.6b01214
J. Phys. Chem. B 2016, 120, 5194–5202

between NO_3^- and C_2mim^+ by H-bonding is stronger than that between NTf_2^- and C_2mim^+. With the increasing ratio of water, more HNO_3 are surrounded by the water molecules and lose

ature Ionic Liquids and the Effect of a Water Impurity. J. Chem. Thermodyn. **2005**, 37, 569−575.
(8) Pandey, S.; Fletcher, K. A.; Baker, S. N.; Baker, G. A. Correlation Between the Fluorescent Response of Microfluidity Probes and the Water Content and Viscosity of Ionic Liquid and Water Mixtures. Analyst **2004**, 129, 569−573.
(9) Inoue, T.; Dong, B.; Zheng, L. Q. Phase Behavior of Binary Mixture of 1-Dodecyl-3-Methylimidazolium Bromide and Water Revealed by Differential Scanning Calorimetry and Polarized Optical Microscopy. J. Colloid Interface Sci. **2007**, 307, 578−581.
(10) Firestone, M. A.; Dzielawa, J. A.; Zapol, P.; Curtiss, L. A.; Seifert, S.; Dietz, M. L. Lyotropic Liquid-Crystalline Gel Formation in a Room-Temperature Ionic Liquid. Langmuir **2002**, 18, 7258−7260.
(11) Billard, I.; Ouadi, A.; Gaillard, C. Liquid-Liquid Extraction of Actinides, Lanthanides, and Fission Products by Use of Ionic Liquids: from Discovery to Understanding. Anal. Bioanal. Chem. **2011**, 400, 1555−1566.
(12) Vasudeva Rao, P. R.; Venkatesan, K. A.; Srinivasan, T. G. Studies on Applications of Room Temperature Ionic Liquids. Prog. Nucl. Energy **2008**, 50, 449−455.
(13) Billard, I.; Gaillard, C. Actinide and Lanthanide Speciation in Imidazolium-Based Ionic Liquids. Radiochim. Acta **2009**, 97, 355−359.
(14) Binnemans, K. Lanthanides and Actinides in Ionic Liquids. Chem. Rev. **2007**, 107, 2592−2614.
(15) Giridhar, P.; Venkatesan, K. A.; Subramaniam, S.; Srinivasan, T. G.; Vasudeva Rao, P. R. Extraction of Uranium (VI) by 1.1 M Tri-n-Butylphosphate/Ionic Liquid and the Feasibility of Recovery by Direct Electrodeposition from Organic phase. J. Alloys Compd. **2008**, 448, 104−108.
(16) Billard, I.; Gaillard, C.; Hennig, C. Dissolution of UO_2, UO_3 and of Some Lanthanide Oxides in BumimTf_2N: Effect of Acid and Water and Formation of $UO_2(NO_3)_3^-$. Dalton Trans. **2007**, 4214−4221.
(17) Billard, I.; Ouadi, A.; Jobin, E.; Champion, J.; Gaillard, C.; Georg, S. Understanding the Extraction Mechanism in Ionic Liquids: UO_2^{2+}/HNO_3/TBP/C_4mimNTf_2 as a Case Study. Solvent Extr. Ion Exch. **2011**, 29, 577−601.
(18) Gaillard, C.; Mazan, V.; Georg, S.; Klimchuk, O.; Sypula, M.; Billard, I.; Schurhammer, R.; Wipff, G. Acid Extraction to a Hydrophobic Ionic Liquid: the Role of Added Tributylphosphate Investigated by Experiments and Simulations. Phys. Chem. Chem. Phys. **2012**, 14, 5187−5199.
(19) Swatloski, R. P.; Visser, A. E.; Reichert, W. M.; Broker, G. A.; Farina, L. M.; Holbrey, J. D.; Rogers, R. D. On the Solubilization of Water with Ethanol in Hydrophobic Hexafluorophosphate Ionic Liquids. Green Chem. **2002**, 4, 81−87.
(20) Freire, M. G.; Carvalho, P. J.; Silva, A. M. S.; Santos, L.; Rebelo, L. P. N.; Marrucho, I. M.; Coutinho, J. A. P. Ion Specific Effects on the Mutual Solubilities of Water and Hydrophobic Ionic Liquids. J. Phys. Chem. B **2009**, 113, 202−211.
(21) Porter, A. R.; Liem, S. Y.; Popelier, P. L. A. Room Temperature Ionic Liquids Containing Low Water Concentrations - a Molecular Dynamics Study. Phys. Chem. Chem. Phys. **2008**, 10, 4240−4248.
(22) Cammarata, L.; Kazarian, S. G.; Salter, P. A.; Welton, T. Molecular States of Water in Room Temperature Ionic Liquids. Phys. Chem. Chem. Phys. **2001**, 3, 5192−5200.
(23) Paul, A.; Mandal, P. K.; Samanta, A. How Transparent are the Imidazolium Ionic Liquids? A Case Study with 1-Methyl-3-Butylimidazolium Hexafluorophosphate, Bmim PF_6. Chem. Phys. Lett. **2005**, 402, 375−379.
(24) Case, D. A.; Darden, T. A.; Cheatham, T. E., III; Simmerling, C. L.; Wang, J.; Duke, R. E.; Luo, R.; Merz, K. M.; Pearlman, D. A.; Crowley, M., et al. AMBER 9; University of California: San Francisco, 2006.
(25) De Andrade, J.; Böes, E. S.; Stassen, H. Computational Study of Room Temperature Molten Salts Composed by 1-Alkyl-3-Methyl-imidazolium Cations—Force-Field Proposal and Validation. J. Phys. Chem. B **2002**, 106, 13344−13351.
(26) Canongia Lopes, J. N.; Pádua, A. A. H. Molecular Force Field for Ionic Liquids Composed of Triflate or Bistriflylimide Anions. J. Phys. Chem. B **2004**, 108, 16893−16898.
(27) Baaden, M.; Burgard, M.; Wipff, G. TBP at the Water-Oil Interface: the Effect of TBP Concentration and Water Acidity Investigated by Molecular Dynamics Simulations. J. Phys. Chem. B **2001**, 105, 11131−11141.
(28) Ryckaert, J. P.; Ciccotti, G.; Berendsen, H. J. C. Numerical-Integration of Cartesian Equations of Motion of a System with Constraints: Molecular Dynamics of N-Alkan1Tf.52936atedChem. Phys.Tf.52938.5(